19. S. Miyakawa, K. Suzuki, T. Noto, Y. Harada, H. Oka-zaki, *J. Antibiot. (Tokyo)* **35**, 411 (1982).
20. R. F. Waller *et al.*, *Proc. Natl. Acad. Sci. U.S.A.* **95**, 12352 (1998).
21. T. L. Doering, M. S. Pessin, G. W. Hart, D. M. Raben, P. T. Englund, *Biochem. J.* **299**, 741 (1994).
22. A. S. Fosbrooke and I. Tamir, *Clin. Chim. Acta* **20**, 517 (1968).
23. M. L. Güther and M. A. Ferguson, *EMBO J.* **14**, 3080 (1995).
24. G. A. Cross, *Parasitology* **71**, 393 (1975).
25. H. Hirumi and K. Hirumi, *J. Parasitol.* **75**, 985 (1989).
26. We thank A. Acosta-Serrano, D. Jiang, M. Klingbeil, D. Lane, T. Shapiro, and P. Watkins for discussions; Y. Ichikawa and V. Klein for help; and Pfizer for thiolac-tomycin. Supported by NIH grant AI21334.

Unfolding Pathways of Individual Bacteriorhodopsins

F. Oesterhelt,[1] D. Oesterhelt,[2] M. Pfeiffer,[2] A. Engel,[3]
H. E. Gaub,[1]* D. J. Müller[3,4]

Atomic force microscopy and single-molecule force spectroscopy were combined to image and manipulate purple membrane patches from *Halobacterium salinarum*. Individual bacteriorhodopsin molecules were first localized and then extracted from the membrane; the remaining vacancies were imaged again. Anchoring forces between 100 and 200 piconewtons for the different helices were found. Upon extraction, the helices were found to unfold. The force spectra revealed the individuality of the unfolding pathways. Helices G and F as well as helices E and D always unfolded pairwise, whereas helices B and C occasionally unfolded one after the other. Experiments with cleaved loops revealed the origin of the individuality: stabilization of helix B by neighboring helices.

Membrane proteins acquire their unique functions through specific folding of their polypeptide chains stabilized by specific interactions in the membrane. Their stability or resistance to unfolding, which goes hand in hand with their anchoring into the hydrophobic belt of the membrane, is usually investigated by chemical or thermal denaturation (*1, 2*). Such experiments, however, provide only ensemble information about the energetics but not about individual proteins and their anchoring forces. As described by the fluid mosaic model (*3*), membrane proteins may diffuse within the bilayer but in the normal direction are strongly restricted to the membrane plane. It is expected that stability of membrane proteins involves interactions with the lipid bilayer as well as intra- and intermolecular interactions (*1*). Thus, it is tempting to determine not only the forces that anchor membrane proteins in the membrane but also the forces that interact between their secondary structure elements.

To answer this pertinent question in membrane biology, we combined atomic force microscopy (AFM) (*4–6*) and single-molecule force spectroscopy (*7–17*) to image individual membrane proteins (*18–21*) and to measure their molecular forces. We chose bacteriorhodopsin (BR), a light-driven proton pump, be-

cause it represents one of the most extensively studied membrane proteins (*22, 23*). Structural analysis has revealed the photoactive retinal embedded in seven closely packed α-helices (*24–28*), which builds a common structural motif among a large class of related G-protein–coupled receptors (*29–32*). Moreover, BR has become a paradigm for α-helical membrane proteins in general and for ion transporters in particular (*22, 23, 33–37*). Together with adjacent lipids, BR molecules assemble into trimers, which are packed into two-dimensional hexagonal lattices, the so-called purple membrane of *Halobacterium salinarum*.

We allowed native purple membrane to adsorb onto a freshly cleaved mica surface (*38*). After being rinsed with buffer, the submolecular resolution of the cytoplasmic purple membrane surface was routinely observed (Fig. 1A) (*39*) in the fluid cell of a commercial AFM. The hexagonal arrangement of the trimeric BR molecules was clearly resolved. Although similar structures can be obtained by electron microscopy and x-ray crystallography, AFM provides structural information about individual proteins and their subunits in aqueous solution (Fig. 1A) (*40*).

After imaging, we positioned the AFM stylus over a protein and pushed it onto the protein with a contact force of ~1 nN for about 1 s. In about 15% of all cases, this resulted in firm adsorption of the protein to the tip, and force extension spectra like the one shown in Fig. 1B were recorded when we retracted the tip (in the other 85% of cases, no attractive interaction was measured upon retraction). The surface was imaged again and, in all cases, we found a vacancy at this position (Fig. 1C), confirming that extraction of a certain individual BR pro-

tein had been recorded in the force spectrum. The fine structure in the force spectra thus contains information about the unfolding process, and the last peak indicates that the extraction is completed.

This experimental protocol ensures that we select and address individual molecules, and it demonstrates the high precision and sensitivity with which we manipulate the protein. However, we do not control which part of the protein interacts with the tip, nor do we have detailed information about the nature of this interaction. In fact, the length of the extracted protein stretch as well as the shape of the force spectra were found to vary significantly, reflecting the variability of the attachment sites. We therefore restricted our data analysis to the 33% of all events in which firm binding of the protein to the tip occurred, which in addition to the imaged vacancy showed a force spectrum with a final rupture peak at the length of an unfolded and fully extended BR. This additional criterion ensures that only those spectra are analyzed in which an individual protein was extracted that was attached to the tip at the cytoplasmic COOH-terminus (see Fig. 2C). Note that 33% is also about what one would expect for random selection of the anchoring point, taking into account that the COOH-terminus covers about one-quarter of the surface of the protein and consists of more than half of all amino acids accessible on the cytoplasmic side (Fig. 4B).

We emphasize that analysis of a selected subset of events from an ensemble is a strength and not a weakness of experiments with individual proteins. In many experiments we can analyze a certain well-defined subset that is characterized by clear criteria and we can investigate correlations within the data (here the position of the last peak with details about the spectrum), which are not accessible in an ensemble average.

A selection of typical unfolding spectra is shown in Fig. 2A. In all cases there are four well-pronounced peaks in predominantly descending order. The relative positions of the second and last peaks are well correlated, but the positions and shapes of the first and the third peaks varied considerably. Superposition of 11 spectra in Fig. 2B reveals that the position of the first peak varies statistically, whereas the third peak appears to be a double peak.

The curves are the calculated force extension relations based on the model shown in Fig. 2C. If we assume that, upon pulling at the cytoplasmic COOH-terminus, helices G and F are extracted and unfolded (diffuse first peak), the protein stretch between the tip and the re-

[1]CeNS and Lehrstuhl für angewandte Physik, Ludwig Maximilians-Universität München, Amalienstrasse 54, 80799 München, Germany. [2]Max-Planck-Institut für Biochemie, Am Klopferspitz 18a, 82152 Martinsried, Germany. [3]M. E. Müller Institute for Structural Biology, Biozentrum, University of Basel, Klingelbergstrasse 70, 4056 Basel, Switzerland. [4]Max-Planck-Insitute of Molecular Cell Biology and Genetics, Pfotenhauerstrasse 108, D-01307 Dresden, Germany.

*To whom correspondence should be addressed.

maining helices in the membrane acts like a polymer spring. The worm-like chain model previously has been shown to provide a very precise description for unfolded proteins. This model has no free parameter: for the Kuhn-length, the elasticity parameter, 0.8 nm was used, a value that was found to hold for a variety of proteins. The contour length was calculated from the known amino acid sequence with a peptide length of 0.36 nm.

The calculated curve describes perfectly the measured extensibility. The increasing force at the slope of the second peak thus reflects the stretching of the already unfolded 88 amino acids of the protein consisting of the intracellular terminal, helices G and F, F–G loops, and E–F loops. Beyond forces of 100 to 200 pN, the remaining membrane anchor is destabilized and yields, which results in a drop in force on the right side of the second peak. Subsequent peaks can be described analogously. The curves were calculated based on the length increase by unfolding of helices E and D for the third peak and of helices C and B for the last peak. Descent of the last peak reflects extraction of helix A. Again, the agreement between theory and data is remarkable. In summary, upon pulling the COOH-terminus of BR, the protein is extracted two helices at a time. It is interesting to note

here that pairwise coupling of the helices was proposed for the insertion process of BR into the membrane by thermodynamic means (41).

The unfolding peaks occur in predominantly descending order. In contrast to unfolding experiments on the muscle protein titin (8) where the maximum force of the peaks is in increasing order, because the weakest of the domains unfolds first, the order of the unfolding events here is determined by the position in the membrane. Missing neighbors destabilize the packing and reduce the anchoring forces of the remaining helices. In control experiments (42), we repeated the extraction experiments on double-layered membrane patches and found no difference. This confirms that the measured extraction forces reflect the membrane anchoring and that contributions of the detachment of the loops from the mica are negligible. Compared with lipids, which at similar loading rates were found to be extracted at forces as low as 25 pN (43), here membrane anchoring of BR was found to be much stronger, presumably because of specific interactions of other than hydrophobic nature (e.g., by inter- and intrahelix hydrogen bonding and interaction with lipids). Because these extraction-unfolding experiments occur under nonequilibrium conditions, the measured forces are rate-dependent. As oth-

ers have shown (8, 9, 43–45), this rate dependence may reveal additional information about basic features of the binding potential. Here we have not analyzed this rate dependence and we have kept the pulling speed constant at 40 nm/s.

In a second set of experiments we selective-

Fig. 2. For analysis, only spectra with maximum length between 60 and 80 nm were selected. (**A**) Several force spectra taken on wild-type BR are shown. A typical repeating pattern is visible. All curves show four peaks located around 10, 30, 50, and 70 nm. (**B**) Thirteen spectra are superposed on the second peak. This results in an exact cover of the third and fourth peaks, whereas the first peak remains scattered. Gray lines are force extension curves calculated by the worm-like chain model with a Kuhnlength of 0.8 nm, which is known to describe the elasticity of an unfolded poly-amino acid chain. The lengths are based on the model shown in (C). (**C**) This model explains the peaks in the force spectra as the sequential extraction and unfolding of a single BR. A rupture length of more than 60 nm can be recorded only if the COOH-terminus has adsorbed on the tip. If a force is applied on the COOH-terminus, helices F and G will be pulled out of the membrane and unfold. Upon further retraction, the unfolded chain will be stretched and a force will be applied on helices D and E until they are extracted from the membrane. Thus, peak 2 reflects unfolding of helices D and E and peak 3 reflects unfolding of helices B and C. Peak 4 shows extraction of the last remaining helix A.

Fig. 1. Controlled extraction of an individual BR from native purple membrane. (**A**) Typical high-resolution AFM topograph of the cytoplasmic surface of a wild-type purple membrane. BR assembles in trimers (for clarity, one is edged with a white line) that arrange in a hexagonal lattice. Purple membranes of *H. salinarum* strain S1 were isolated as described (49). A stock solution of protein (5 mg/ml) was kept in ultrapure water at 4°C. The AFM used was a Nanoscope III (Digital Instruments, Santa Barbara, California) equipped with a J-scanner (80 μm) and oxide-sharpened Si_3N_4 tips on a cantilever (Olympus, Tokyo). The spring constant of the cantilevers as estimated by analysis of the thermal noise spectra was 0.1 N/m. All experiments were done in buffer solution (300 mM KCl, 10 mM tris-HCl, pH 7.8) at room temperature. To catch an individual protein (white circle), we zoomed in by reducing the frame size and the number of pixels. After the tip was positioned, it was kept in contact with the selected protein for about 1 s while a force of ~1 nN was applied to give the protein the chance to adsorb on the stylus. (**B**) The stylus and protein surface were separated at a velocity of 40 nm/s while the force spectrum was recorded (512 or 4096 pixels). The interaction between tip and surface, which is expressed in the marked discontinuous changes in the force, indicates a molecular bridge between tip and sample. This bridge reaches far out to distances up to 75 nm, which corresponds to the length of one totally unfolded protein. (**C**) After the

adhesive force peaks were recorded, a topograph of the same surface was taken to show structural changes. Note that a single monomer is missing (white circle). Thus, the recorded force spectrum may be correlated to extraction of an individual protein from the membrane. The defect at the lower rim was taken to correlate both topographs. The full gray-level range of the topographs is 1.5 nm. For this procedure, the drift of the microscope had to be minimized by thermal relaxation as indicated by the image shift, which was less than 5 nm/min.
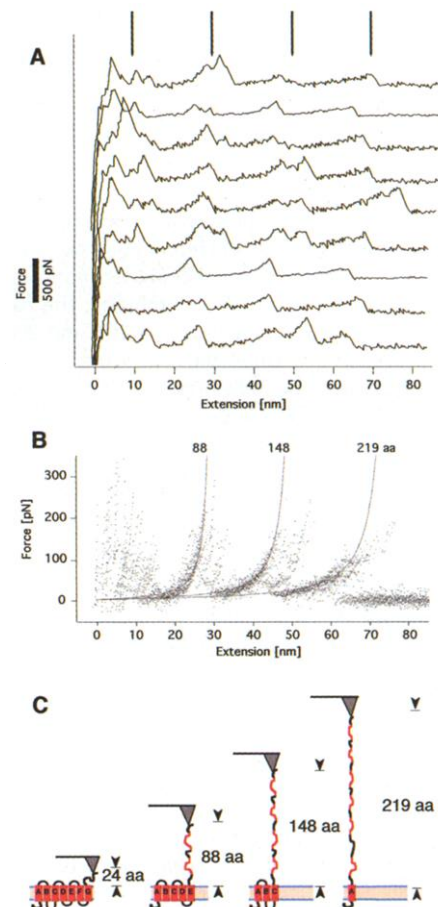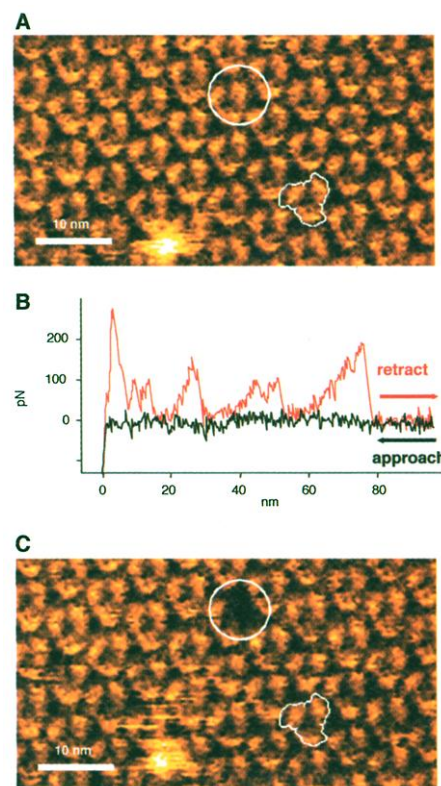
ly cleaved the E–F loop (see Fig. 3C) and repeated the measurements described above. For those experiments, we used a genetically engineered mutant in which specific cleavage sites for protease V8 were introduced in the E–F loop. Introducing the cleavage sites and cleaving the loop do not influence the functionality and structure of the protein (46). The first striking result was that we found no force spectra longer then 45 nm. We then analyzed all spectra that reached a length of 40 nm, which occurred in 25% of all cases in which there was firm binding of the protein to the tip. This way we exclusively selected molecules that were attached to the tip with helix E. Representative
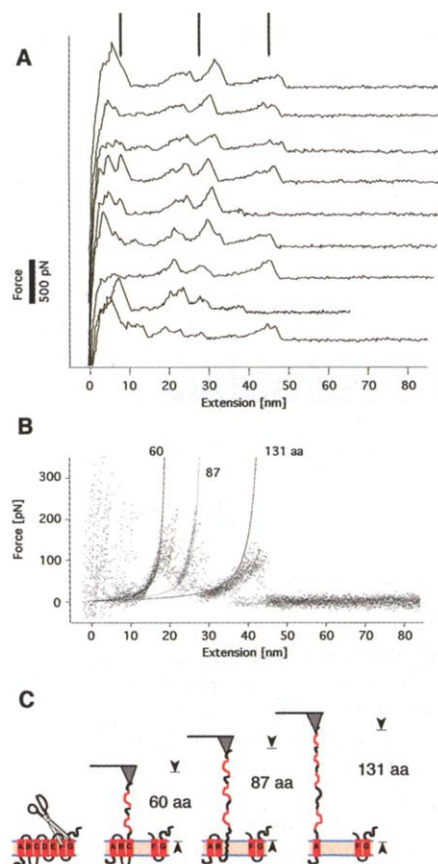

force spectra are shown in Fig. 3A. Superposition of 17 curves (Fig. 3B) clearly reveals that the unfolding pattern is shifted by one peak to shorter lengths. Calculated curves, based on the model shown in Fig. 3C, were superimposed again. The last peak at 40 nm again is perfectly consistent with stretching of the fully unfolded helices B, C, D, and E and the corresponding loops. The descending side of the peak reflects unfolding and extraction of helix A, which results in final detachment. The peak at 18 nm reflects stretching of unfolded helices D and E together with the corresponding loops, and its descending side reflects unfolding and extraction of helices B and C. Helices D and E are extracted in the diffuse peak at the beginning. In fact the first peak, the unfolding of helices F and G, which now remain in the membrane, is the one that is missing.

In addition to the unfolding pattern of the native protein, we found a well-pronounced structure in-between these two peaks on the membrane with the cleaved E–F loop. This means that details of the unfolding pathway of helices B and C are resolved and that this pathway differs from the pathway in the uncleaved protein. The curve, which fits the elastic side of the intermediate peak, was calculated based on the assumption that helix B remains intact and that only helices C, D, and E and the connecting loops are stretched. While subsequent extraction and unfolding of helix B, which is reflected in the sharp drop, appears to be an all-or-none process, extraction and unfolding of helix C follows a complex path. This is reflected in the finding that the force does not drop to the baseline but stays at about 100 pN, which means that this helix unfolds gradually. Thus, throughout successive unfolding of helix C, the interaction of the amino acids must remain at a high level, which requires the structures surrounding this helix to remain preserved. The faint fine structure in this plateau, which contains further details about the unfolding process, is at the resolution limit of our

instrument and is not discussed here. In summary, after helices E and D are extracted as a pair, helix C unfolds step by step and then helix B proceeds in an all-or-none manner.

The finding that helices C and B follow different unfolding patches in the different membranes is best understood in view of the three-dimensional structure sketched in Fig. 4. In the native membrane, helices G and F are already unfolded when helices B and C are extracted. In the cleaved membrane, helices G and F are still in position, preserving the structure and providing stabilizing interactions to helices B and C. Upon unfolding, these local interactions must be overcome and result in the fine structures in the measured force spectra. A close look at Fig. 2B reveals that, in rare cases, this intermittent unfolding pathway also is taken by the uncleaved protein in the membrane. One might speculate that helix A remains stabilized by helices F and G because the drop of the last peak occurs suddenly in the wild type, unlike the gradual descent in the cleaved membrane.

For an additional control, we repeated the measurements with the mutant G241C, which has a cysteine instead of glycine in the COOH-terminus at position 241 (47, 48); we contacted this with a gold-coated AFM tip to form a specific linkage. Unfortunately, because of the high adsorbance of proteins to gold surfaces, contamination prohibited high-resolution imaging and thus confirmation of individual manipulation by imaging the resulting vacancies. But we measured a site-specific single molecule attachment in more than 80% of all contacts. The remaining 20% are predominantly multiple interactions. The resulting force spectra fully corroborate our previous experiments and show even more details that support our previous interpretation (Fig. 5).

Mechanical manipulation of selected molecules (e.g., by force spectroscopy in combination with high-resolution imaging) is an extremely powerful approach, which in this study has revealed a very detailed map of the unfold-
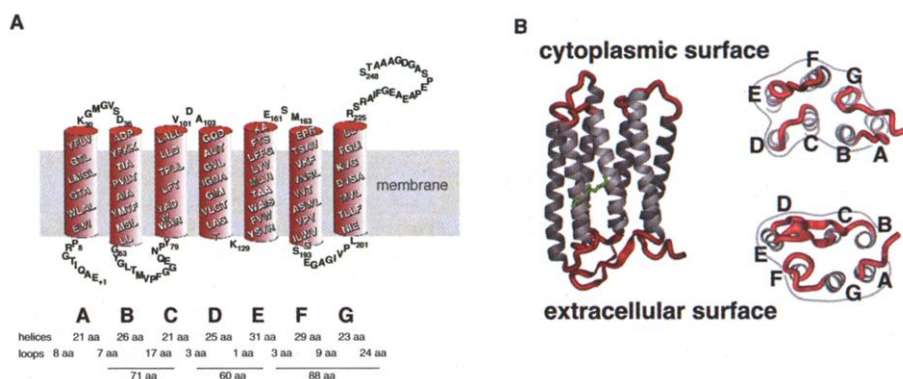
Fig. 3. Force curves were recorded on BR where the E–F loop was cleaved enzymatically. (**A**) Selection of the longest force curves taken on the cleaved BR. No recorded spectrum showed a rupture length beyond 50 nm. Only three main peaks are visible—around 5, 25, and 45 nm—and the second is a double peak. (**B**) Superposition of 17 spectra on the second peak results in an exact cover of all but the first peak. Gray lines are force extension curves calculated by the WLC model as in Fig. 2B. (**C**) Because loop F–G is cut out, force curves with a length of 45 nm can be recorded only when the free end of helix E is fixed to the tip. Thus, the first peak reflects extraction of helices D and E and the second reflects extraction and unfolding of helices B and C; the last peak shows extraction of the last remaining helix A. Consequently, the intermediate peak between peaks 2 and 3 reflects stepwise unfolding of helices A and B.

Fig. 4. Model of the three-dimensional structure of BR. (**A**) BR is a 248–amino acid membrane protein that consists of seven transmembrane α-helices, which are connected by loops. (**B**) Three-dimensional model and top and bottom view show spatial arrangement of the helices. Helices F and G are neighboring helices A and B and thus can stabilize them.
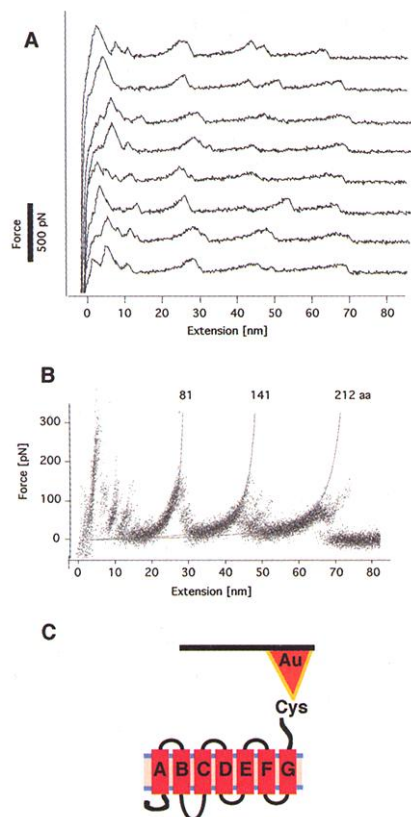
Fig. 5. (A) Force spectra of BR mutant G241C with specific anchoring of the COOH-terminus. In G241C, a terminal cysteine was introduced near the COOH-terminus at position 241, allowing specific attachment to a gold evaporated tip. In these experiments, the percentage of full-length force curves increased to 80%. (B) Thirty-five force curves are superposed and WLC fits with lengths corresponding to the model shown in Fig. 2 are drawn. In contrast to the measurements in which we used unspecific attachment, we also could resolve the substructure of the first peak, which reflects unfolding of helices F and G.

ing pathways and the local interactions within this membrane protein. In particular, the combination of imaging and spectroscopy enabled us to unravel the individualism of the unfolding processes. Better instruments should allow an even more detailed interpretation of the unfolding pathways of a broad range of membrane proteins such as G proteins and ion channels.

References
1. T. Haltia and E. Freire, *Biochim. Biophys. Acta Bioenerg.* **1228**, 1 (1995).
2. S. H. White and W. C. Wimley, *Annu. Rev. Biophys. Biomol. Struct.* **28**, 319 (1999).
3. S. J. Singer and G. L. Nicolson, *Science* **175**, 720 (1972).
4. G. Binnig, C. F. Quate, C. Gerber, *Phys. Rev. Lett.* **56**, 930 (1986).
5. M. Radmacher, R. W. Tillmann, M. Fritz, H. E. Gaub, *Science* **257**, 1900 (1992).
6. B. Drake *et al.*, *Science* **243**, 1586 (1989).
7. M. Rief, F. Oesterhelt, B. Heymann, H. E. Gaub, *Science* **275**, 1295 (1997).
8. M. Rief, M. Gautel, F. Oesterhelt, J. M. Fernandez, H. E. Gaub, *Science* **276**, 1109 (1997).
9. R. Merkel, P. Nassoy, A. Leung, K. Ritchie, E. Evans, *Nature* **397**, 50 (1999).
10. D. J. Müller, W. Baumeister, A. Engel, *Proc. Natl. Acad. Sci. U.S.A.* **96**, 13170 (1999).
11. A. F. Oberhauser, P. E. Marszalek, H. P. Erickson, J. M. Fernandez, *Nature* **393**, 181 (1998).
12. S. B. Smith, Y. Cui, C. Bustamante, *Science* **271**, 795 (1996).
13. P. Hinterdorfer, W. Baumgartner, H. J. Gruber, K. Schilcher, H. Schindler, *Proc. Natl. Acad. Sci. U.S.A.* **93**, 3477 (1996).
14. U. Dammer *et al.*, *Biophys. J.* **70**, 2437 (1996).
15. U. Dammer *et al.*, *Science* **267**, 1173 (1995).
16. E.-L. Florin, V. T. Moy, H. E. Gaub, *Science* **264**, 415 (1994).
17. G. U. Lee, L. A. Chris, R. J. Colton, *Science* **266**, 771 (1994).
18. A. Engel, H. Gaub, D. J. Müller, *Curr. Biol.* **9**, R133 (1999).
19. A. Engel, C.-A. Schoenenberger, D. J. Müller, *Curr. Opin. Struct. Biol.* **7**, 279 (1997).
20. Y. Zhang, S. Sheng, Z. Shao, *Biophys. J.* **71**, 2168 (1996).
21. Z. Shao and J. Yang, *Q. Rev. Biophys.* **28**, 195 (1995).
22. U. Haupts, J. Tittor, D. Oesterhelt, *Annu. Rev. Biophys. Biomol. Struct.* **28**, 367 (1999).
23. D. Oesterhelt, *Curr. Opin. Struct. Biol.* **8**, 489 (1998).
24. N. Grigorieff, T. A. Ceska, K. H. Downing, J. M. Baldwin, R. Henderson, *J. Mol. Biol.* **259**, 393 (1996).
25. Y. Kimura *et al.*, *Nature* **389**, 206 (1997).
26. E. Pebay-Peyroula, G. Rummel, J. P. Rosenbusch, E. M. Landau, *Science* **277**, 1676 (1997).
27. L.-O. Essen, R. Siegert, W. D. Lehmann, D. Oesterhelt, *Proc. Natl. Acad. Sci. U.S.A.* **95**, 11673 (1998).
28. H. Luecke, H.-T. Richter, J. K. Lanyi, *Science* **280**, 1934 (1998).
29. E. J. M. Helmreich and K.-P. Hofmann, *Biochim. Biophys. Acta* **1286**, 285 (1996).
30. J. M. Baldwin, *EMBO J.* **12**, 1693 (1993).
31. P. A. Hargrave, *Curr. Opin. Struct. Biol.* **1**, 575 (1991).
32. R. Henderson, F. R. S. Shertler, G. F. X. Shertler, *Philos. Trans. R. Soc. London Ser. B* **326**, 379 (1990).
33. J. K. Lanyi, *J. Biol. Chem.* **272**, 31209 (1997).
34. ———, *Nature* **375**, 461 (1995).
35. ———, *Biochim. Biophys. Acta* **1183**, 241 (1993).
36. H. Luecke, B. Schobert, H. Richter, J. Cartailler, J. Lanyi, *Science* **286**, 255 (1999).
37. ———, *J. Mol. Biol.* **291**, 899 (1999).
38. D. J. Müller, M. Amrein, A. Engel, *J. Struct. Biol.* **119**, 172 (1997).
39. D. J. Müller, D. Fotiadis, S. Scheuring, S. A. Müller, A. Engel, *Biophys. J.* **76**, 1101 (1999).
40. D. J. Müller, H.-J. Sass, S. Müller, G. Büldt, A. Engel, *J. Mol. Biol.* **285**, 1903 (1999).
41. D. M. Engelman and T. A. Steitz, *Cell* **23**, 411 (1981).
42. Data not shown.
43. E. Evans and F. Ludwig, *J. Phys. Condens. Matter* **11**, 1 (1999).
44. M. Rief, J. M. Fernandez, H. E. Gaub, *Phys. Rev. Lett.* **81**, 4764 (1998).
45. H. Grubmüller, B. Heymann, P. Tavan, *Science* **271**, 997 (1995).
46. J. B. Heymann *et al.*, *Structure*, in press.
47. M. Pfeiffer, dissertation, Ludwig-Maximilians-Universität München (2000).
48. M. Pfeiffer, T. Rink, K. Gerwert, D. Oesterhelt, H.-J. Steinhoff, *J. Mol. Biol.* **287**, 163 (1999).
49. D. Oesterhelt and W. Stoeckenius, *Methods Enzymol.* **31**, 667 (1974).

Specification of *Drosophila* Hematopoietic Lineage by Conserved Transcription Factors

Tim Lebestky,[1]* Ting Chang,[2]* Volker Hartenstein,[1,2] Utpal Banerjee[1,2,3]†

Two major classes of cells observed within the *Drosophila* hematopoietic repertoire are plasmatocytes/macrophages and crystal cells. The transcription factor Lz (Lozenge), which resembles human AML1 (acute myeloid leukemia–1) protein, is necessary for the development of crystal cells during embryonic and larval hematopoiesis. Another transcription factor, Gcm (glial cells missing), has previously been shown to be required for plasmatocyte development. Misexpression of Gcm causes crystal cells to be transformed into plasmatocytes. The *Drosophila* GATA protein Srp (Serpent) is required for both Lz and Gcm expression and is necessary for the development of both classes of hemocytes, whereas Lz and Gcm are required in a lineage-specific manner. Given the similarities of Srp and Lz to mammalian GATA and AML1 proteins, observations in *Drosophila* are likely to have broad implications for understanding mammalian hematopoiesis and leukemias.

Hematopoietic stem cells give rise to all blood cell lineages in mammals (*1*). Molecular decisions that differentiate one lineage from another are regulated by unique protein complexes constituted of general as well as lineage-specific transcription factors (*2*). Gene inactivation studies in mice have identified an important role for a number of hematopoietic transcription factors. For example, GATA-1 is required for erythroid development (*3*), GATA-2 for definitive hematopoiesis (*4*), and GATA-3 for T cell development (*5*). Interestingly, the *Drosophila* GATA homolog *serpent* (*srp*) is required for embryonic blood cell development (*6*). Another mammalian gene, encoding the AML1 protein, is the most frequent target of chromosomal

---

[1]Molecular Biology Institute, [2]Department of Molecular, Cell, and Developmental Biology, [3]Departments of Biological Chemistry and Human Genetics, University of California, Los Angeles, CA 90095, USA.

*These authors contributed equally to this report.
†To whom correspondence should be addressed. E-mail: banerjee@mbi.ucla.edu